Laser propagation in cylindrical waveguides

J. R. Davies and J. T. Mendonça
GoLP, Instituto Superior Técnico, 1049-001 Lisboa, Portugal
(Received 21 May 2002; published 9 October 2002)

Laser propagation in cylindrical waveguides is studied theoretically, assuming that the guide medium and the internal medium have permittivities and identical permeabilities that are uniform in space and time and independent of the fields. Approximate solutions to the cylindrical dispersion relation are found and compared with numerical solutions. For high refractive indices and small radii the modes are transverse electric and transverse magnetic, as in the loss-less case. As the refractive index is lowered or the radius increased the lower-order modes become hybrid electric and hybrid magnetic, and the lower-order transverse magnetic modes are modified. The higher-order modes, in any waveguide, are always transverse. The transition to hybrid modes is marked by the disappearance of the fundamental electric mode and the appearance of an additional magnetic mode. This mode and the losses of the magnetic modes adjacent to it are only adequately described by numerical solutions. The losses of the transverse modes are accurately reproduced by a simple model based on a mean reflectivity.

DOI: 10.1103/PhysRevE.66.046604 PACS number(s): 42.79.Gn, 52.38.−r

I. INTRODUCTION

Propagating a laser pulse in a cylindrical waveguide (capillary tube) has been proposed as a means of guiding the ignition pulse to the target in alternative fast ignition schemes [1], as a means of extending the interaction length with a gas [2,3] or an under dense plasma [4], of particular interest to laser-plasma accelerators, as a means of creating a long scale length plasma [4,5] and as a new method of accelerating and focusing electrons [6], using the conical plasma front created by ablation of the wall. A number of experimental results on laser propagation in cylindrical waveguides have been published [1,4,5,7]. The subject of this paper is the theory of laser propagation in cylindrical waveguides; we will not consider the plasma creation aspect. In a previous paper [8] we showed how the essential features of wave propagation in hollow waveguides can be derived from the basic physical model of waves reflecting between the guide walls. We estimated the losses in cylindrical waveguides in terms of an arbitrary reflectivity, using the loss-less solution to obtain the angle of incidence and polarization of the incident waves at the wall. The advantage of this approach is that the reflectivity can be taken from any theoretical model or experimental results. It is a generalization of the method based on the surface impedance, commonly used in microwave applications [9]. The disadvantage is that it is based on the loss-less solutions, and the validity of this assumption cannot be determined from the model itself. In this paper we consider the case in which the guide medium and the internal medium can be represented by permittivities and a single permeability that are uniform in space and time and independent of the fields. The solutions of Maxwell's equations in this case are well known, but the cylindrical dispersion relation cannot be solved analytically. Here we will attempt to find approximate solutions, informed by numerical solutions. Approximate solutions have been given by other authors [10,11], however, as we will see, these treatments are incomplete and of limited validity. As the equations and their derivations are well known, and have been discussed in many books and articles, e.g., Refs. [8–11], we will only briefly outline the steps used in deriving them and we will not explicitly consider the fields.

II. FORMULATING THE PROBLEM

We consider an infinitely long, cylindrical waveguide with infinitely thick walls and internal radius a. We look for wave mode solutions to Maxwell's equations with angular frequency ω, traveling in the axial (z) direction with fixed azimuthal (θ) and radial (r) profiles. The fields then have the form

$$\mathbf{E},\mathbf{B}\propto\mathbf{F}(k_\perp r)e^{i(n\theta+\omega t-k_z z)}, \tag{1}$$

where $\boldsymbol{F}$ is a function that is to be determined for each of the field components, $k_\perp$ is the wave number perpendicular to the axis, which is to be determined, n, the azimuthal mode number, is an integer $\geqslant 0$, and k_z is the axial wave number. This is determined by the wave number $k=\omega c$, where c is the speed of light in the medium, and the perpendicular wave number from $k_z^2=k^2-k_\perp^2$. As $|k|>|k_\perp|$ is required for a mode to propagate, $k_\perp$ is often referred to as the cutoff wave number (k_c) [8,9]. It is useful to introduce a dimensionless form

$$u=k_\perp a. \tag{2}$$

The parameters u, k_z, k, and c are, in general, complex. The imaginary part of k_z, $k_{z\Im}$, is the loss term. It has two components; $k_{\Re}k_{\Im}/k_{z\Re}$, which gives the losses due to dissipation in the medium, and $-u_{\Re}u_{\Im}/(k_{z\Re}a^2)$, which gives the losses due to radial divergence. Inside the guide, this gives the losses to the wall. The equations for the radial dependence of the field components, $F(ur/a)$, are naturally expressed in terms of the axial fields [9], since the fields perpendicular to the axis can be determined from the axial fields and there does not exist a solution without one or other of the axial field components [8,9]. The radial dependence of the axial field components is given by Bessel's differential equation.

Inside the guide we assume a superposition of waves reflected from opposite points of the guide wall and take the solution in terms of the Bessel functions J_n. In the guide wall we assume that there is only a radially diverging wave and take the solution in terms of Hankel functions of the second kind, which we will write simply as H_n, as we will not be concerned with the first kind. The values of u and the relative amplitudes of the axial field components are then determined from the boundary conditions. The values of k_z and ω must be the same inside the guide and in the guide wall, so u in the guide wall, which we will denote u_g, is determined by u and k inside the guide from

$$u_g^2=(\nu^2-1)k^2a^2+u^2, \tag{3}$$

where $\nu=c/c_g$ is the refractive index. We assume that $|\nu|>1$ and that its imaginary component $\nu_\Im \leqslant 0$. Before giving the results for the general case, we will consider the case in which there are no losses to the wall, as the solution is known. This corresponds to the limit $|\nu|\to\infty$. The solution has two classes of modes, one with no axial electric field, called transverse electric, and the other with no axial magnetic field, called transverse magnetic. The transverse electric modes are labeled TE_{nm} and have $u=u'_{nm}$, where $J'_n(u'_{nm})=0$, J'_n indicating the derivative of J_n, and m, the radial mode number, is an integer >0 that denotes the succesive roots of the equation. The transverse magnetic modes are labeled TM_{nm} and have $u=u_{nm}$, where $J_n(u_{nm})=0$. We will refer to this solution as the loss-less solution, even though there may be losses to the internal medium. We described the fields and intensities of these modes in our previous paper [8], and they are considered, from a somewhat different point of view, by Elliot [9]. For a finite refractive index, the solutions contain, in general, both axial field components, and are referred to as hybrid modes. We will consider these to consist of transverse electric and transverse magnetic components. The value of u is determined by the cylindrical dispersion relation [10,11]. As we know that the solution has separate transverse electric and transverse magnetic modes as limits, we introduce the form

$$D^2=D_{TE}D_{TM}-S^2=0, \tag{4}$$

where

$$D_{TE}=J'_n(u)H(u_g)-\frac{u}{u_g}J_n(u)H'_n(u_g) \tag{5}$$

gives the dispersion relation for transverse electric modes,

$$D_{TM}=J'_n(u)H(u_g)-\nu^2\frac{u}{u_g}J_n(u)H'_n(u_g) \tag{6}$$

gives the dispersion relation for transverse magnetic modes, and

$$S=\frac{n}{u}J_n(u)H_n(u_g)\sqrt{1-\frac{u^2}{u_g^2}}\sqrt{1-\nu^2\frac{u^2}{u_g^2}} \tag{7}$$

determines the separation of the components. In writing the dispersion relation in this form we have taken care not to divide by parameters that may go to zero. The ratio of the amplitudes of the transverse electric (A_{TE}) and transverse magnetic (A_{TM}) components is given by

$$\frac{A_{TE}}{A_{TM}}=i\frac{S}{D_{TE}}=i\frac{D_{TM}}{S}. \tag{8}$$

Note that for the amplitude of the magnetic field to have the same units as that of the electric field it is necessary to divide the magnetic field by the speed of light in the medium, a convention we used in our previous paper [8]. The ratio of the amplitudes of the fields in the guide wall (A_g) to that inside the guide (A) is given by

$$\frac{A_g}{A}=\frac{J_n(u)}{H_n(u_g)}. \tag{9}$$

For a more detailed derivation and discussion of these results see Cros *et al.* [11]. We cannot solve the cylindrical dispersion relation [Eq. (4)] analytically, so we look for approximate solutions and compare them with numerical solutions.

III. TRANSVERSE SOLUTIONS

First we consider under what circumstances we have, approximate, transverse electric and transverse magnetic modes, that is when $S\approx 0$ [Eq. (7)], and find approximate solutions for these modes. The first term in S, n/u, is identically zero for $n=0$ and approximately zero for $|u|\gg n$, which applies to modes with high radial mode numbers, $m\gg 1$; n/u is relatively insensitive to the value of n. The second term, $J_n(u)$, vanishes when $u=u_{nm}$, which is the case for the loss-less transverse magnetic modes. As we will see later, this holds when $|\nu^2 u|\gg|u_g|$. The third term, $H_n(u_g)$, vanishes as $|\nu|\to\infty$, the limit in which we expect to have transverse modes. The fourth term, $1-u^2/u_g^2$, is never close to zero, as $|u_g|>|u|$ [Eq. (3)]. The last term, $1-\nu^2u^2/u_g^2$, goes to zero as u approaches ka, in other words close to cutoff, and is identically zero at cutoff when $u=ka$.

The dispersion relations for the transverse electric and transverse magnetic modes, Eqs. (5) and (6), can be solved approximately as in our previous paper [8]. We divide by $J_n(u)H_n(u_g)$ and use the approximation $H'_n(u_g)/H_n(u_g)\approx -i$ for $|u_g|\gg 1$. This approximation is far more accurate than either the large argument forms of H'_n or H_n. It only breaks down for high values of n. We then look for a solution of the form $u=u_0+\Delta u$, such that $|\Delta u|\ll 1$, by expanding $J_n(u)$ and $J'_n(u)$ about u_0 to first order in Δu using Taylor's theorem. Expanding u_g to first order in Δu gives $u_g\approx u_{g0}+\Delta u\, u_0/u_{g0}$, where

$$u_{g0}^2=(\nu^2-1)k^2a^2+u_0^2. \tag{10}$$

The obvious values to try for u_0 are the values of u from the loss-less solution given in Sec. II. For the transverse electric modes we obtain a solution with $u_0=u'_{nm}$ provided $u_0\ll|u_{g0}|$,

$$\Delta u_{TE} \approx i \frac{1}{1-n^2/u_0^2} \frac{u_0}{u_{g0}}. \tag{11}$$

Comparing Eqs. (5) and (6) we see that $u_0 = u'_{nm}$ will also give an acceptable solution for the transverse magnetic modes provided $|\nu^2| u_0 \ll |u_{g0}|$, giving

$$\Delta u_{TM} \approx \nu^2 \Delta u_{TE}, \ |\nu^2| u_0 \ll |u_{g0}|. \tag{12}$$

We introduce the notation TM'_{nm} for these modes, to distinguish them from the loss-less modes. For u_0 equal to the loss-less solution, u_{nm}, to give an acceptable solution requires $|\nu^2| u_0 \gg |u_{g0}|$. In this case we divide Eq. (6) by $J'_n(u)$ instead of $J_n(u)$ and obtain

$$\Delta u_{TM} \approx i \frac{u_{g0}}{\nu^2 u_0}, \ \ |\nu^2| u_0 \gg |u_{g0}|. \tag{13}$$

For intermediate values of $|\nu^2| u_0 / |u_{g0}|$ we cannot find a solution for the transverse magnetic modes by this method, so this completes the approximate transverse solutions.

IV. HYBRID SOLUTIONS

We now consider hybrid solutions. These require $n > 0$ and $|\nu^2 u| \ll |u_g|$, therefore $S \approx n/u$. Again using $H'_n(u_g)/H_n(u_g) \approx -i$, we write the dispersion relation [Eq. (4)] as a quadratic in $J'_n(u)/J_n(u)$, which we abbreviate as x,

$$x^2 + i(\nu^2 + 1) \frac{u}{u_g} x - \nu^2 \frac{u^2}{u_g^2} - \frac{n^2}{u^2} \approx 0. \tag{14}$$

Marcatili and Schmeltzer [10] and Cros *et al.* [11] give hybrid solutions with $u_0 = u_{n-1m}$, giving $x \approx -\Delta u - n/u$. As we will see from the solution, u/u_g and n/u are of order Δu, so every term in Eq. (14) is second order and we obtain

$$\Delta u_{HM} \approx i \frac{\nu^2 + 1}{2} \frac{u_0}{u_{g0}} - \frac{n}{u_0} (1 - \sqrt{1 - \overline{S^2}}) \tag{15}$$

and

$$\frac{A_{TE}}{A_{TM}} \approx -\overline{S} - i\sqrt{1 - \overline{S^2}}, \tag{16}$$

where

$$\overline{S} = \frac{(\nu^2 - 1) u_0^2}{2 n u_{g0}}. \tag{17}$$

$|\Delta u| \ll 1$ requires $|\nu^2| u_0 \ll |u_{g0}|$, as we assumed at the outset. The parameter $\overline{S}$ contains the reciprocal of all the essential "separation" factors in S [Eq. (7)] discussed at the beginning of Sec. III, hence the notation. It is the pivotal result of this paper, determing the validity of previous hybrid solutions [10,11] and treatments based on the loss-less solutions [8,9]. For $|\overline{S^2}| \ll 1$ the amplitudes of the transverse electric and transverse magnetic components [Eq. (16)] are approximately equal and Δu [Eq. (15)] is approximately the average of the transverse electric and transverse magnetic results of Eqs. (11) and (12). For $|\overline{S^2}| \gg 1$, the amplitude of the transverse electric component vanishes and Δu tends to the transverse magnetic result of Eq. (12). Thus we christen these modes hybrid magnetic, labeling them HM_{nm}, to be consistent with the notation of the transverse modes TM_{nm}. Cros *et al.* [11] discuss these modes, which they call electric hybrid modes EH_{nm} in some detail, for $|\overline{S^2}| \ll 1$. They consider Δu to zeroth order in $\overline{S}$ and A_{TE}/A_{TM} to first order. This is quite a restrictive assumption, as we can see by rewriting $\overline{S}$, using $u_{g0} \approx \sqrt{\nu^2 - 1}\, ka$ [Eq. (10)], which is a good approximation for the hybrid modes, as

$$\overline{S} \approx \frac{1}{2} \sqrt{\nu^2 - 1} \frac{u_0}{n} \frac{u_0}{ka}. \tag{18}$$

Both $|\nu^2 - 1|$ and u_0/n are greater than unity and, for a propagating mode, u_0 may have values up to ka, therefore the assumption $|\overline{S^2}| \ll 1$ breaks down in all waveguides. As an example, consider an evacuated glass waveguide with $\nu = 1.5$ and $ka = 100$, for $n = 1$, $\overline{S} < 1$ only applies up to $m = 4$, and $n = 1$ modes up to $m = 32$ could propagate.

The transition of the hybrid magnetic solution [Eq. (15)] to the transverse magnetic solution [Eq. (12)] is not a smooth one because the value of u_0 decreases from u_{n-1m} in Eq. (15) to u'_{nm} in Eq. (12). Furthermore, for $|\nu^2| u_0 > |u_{g0}|$, which occurs in all waveguides, u_0 increases to u_{nm} and Δu is given by Eq. (13). We have three different solutions for three different regimes. Numerical solutions indicate that for $|\overline{S}| < 1$ the hybrid solutions, $u_0 = u_{n-1m}$, are a good approximation and that for $|\overline{S}| > 1$ the transverse solutions are the best approximation. For $|\nu^2| u_0 < |u_{g0}|$ the transverse modes have $u_0 = u'_{nm}$ and for $|\nu^2| u_0 > |u_{g0}|$ they have $u_0 = u_{nm}$. However, Eqs. (12) and (13) are only accurate for small and large values of $|\nu^2| u_0 / |u_{g0}|$, respectively. A difference of about a factor of 2 between $|\nu^2| u_0$ and $|u_{g0}|$ is sufficient for the approximations to give accurate results. For intermediate values, $u_{\Im}$ is significantly underestimated. As $u_{\Re}$ is dominated by u_0, it is accurately predicted for all of the modes.

To reproduce the loss-less results there must also be hybrid electric modes HE_{nm} and Eq. (14) certainly has two solutions. The obvious value of u_0 for these modes is u'_{nm}, giving $x \approx -\Delta u (1 - n^2/u_0^2)$ and

$$\Delta u_{HE} \approx \frac{1}{1 - n^2/u_0^2} \left(i \frac{\nu^2 + 1}{2} \frac{u_0}{u_{g0}} - \frac{n}{u_0} \sqrt{1 - \overline{S^2}} \right) \tag{19}$$

with

$$\frac{A_{TM}}{A_{TE}} \approx -\overline{S} - i\sqrt{1 - \overline{S^2}}, \tag{20}$$

which satisfy all of the conditions we require for hybrid electric modes. Marcatili and Schmeltzer [10] consider the fields of these modes, which they call electric hybrid modes EH_{nm}

for $|\overline{S^2}| \ll 1$ and $u_0 \gg n$. However, as a result of their approximations, they obtained the hybrid magnetic result for u [8].

The hybrid electric solution [Eq. (19)] shows a smooth transition to the transverse electric solution [Eq. (11)] as $\overline{S}$ increases. Equation (19) does not require $|\nu^2| u_0 \ll |u_{g0}|$ to ensure $|\Delta u| \ll 1$, $u_0 \ll |u_{g0}|$ is sufficient. Numerical solutions indicate that Eq. (19) is more accurate than Eq. (11) for the first few modes with $|\overline{S}| > 1$, and for higher values of $|\overline{S}|$ there is no significant difference between the two results. As we have $u_0/|u_{g0}| < 1/|\nu|$ for a propagating mode, Eq. (19) only breaks down for low-refractive indices near cutoff, where it underestimates $u_\Im$. However, for almost all cases of interest, the error is not significant. Equation (19) is an adequate approximation for all of the $n > 0$ electric modes, with one important exception. There are no $m = 1$ hybrid electric modes. For $m = 1$, Eq. (19) does not satisfy $|\Delta u| \ll 1$, because $u'_{n1} \sim n$, the values getting closer as n increases. Numerical solutions for values of n from 1 to 5 confirmed that there are no $m = 1$ hybrid electric modes. There will only be $m = 1$ transverse electric modes with $n > 0$ when $|\overline{S}| > 1$ for this mode or when the $m = 1$ hybrid magnetic mode is cutoff. As we mentioned in Sec. III, for $n = 0$ the modes are purely transverse. This means that the fundamental hybrid mode, that is the mode with the lowest value of u_0, is the HM_{11} mode ($u_0 \approx 2.405$), not the HE_{11} mode ($u_0 \approx 1.841$), whose transverse equivalent TE_{11} is *the* fundamental mode. The disappearance of what should be the fundamental hybrid mode means that we do not have an approximate general solution to Maxwell's equations: we cannot represent an arbitrary radial profile inside the guide with the hybrid modes that actually exist. We only have a complete solution when the $m = 1$ transverse electric modes exist.

V. NUMERICAL EXAMPLES

We will now give an example of the numerical results for $\nu = 1.5$, $ka = 20$, and $n = 1$. This corresponds to an evacuated glass waveguide with a rather small radius, but it allows us to demonstrate all of the important transitions in a handful of modes. We chose $n = 1$ as this corresponds to typical laser pulses. For this refractive index we have considered values of ka from 1.8 to 100 and values of n from 0 to 5. All of these results showed the same features we describe here. Given that the refractive index of dielectrics varies from about 1.4 to around 2.1 [9], these results can be taken as representative of dielectric waveguides. We consider the absolute value of D [Eq. (4)] in the complex u plane ($u_\Re, u_\Im$), looking for the position of the minima. These are plotted as filled circles in Fig. 1. They were obtained using a grid spacing of 10^{-3} in $u_\Re$ and 10^{-4} in $u_\Im$ [12]. The grid lines in $u_\Re$ give the values of u'_{1m}, u_{0m}, and u_{1m}, which appear in that order. However, the values of u'_{1m} and u_{0m} are so close for $m > 2$ that only the values of u'_{1m} are actually shown. The solid vertical lines give the positions of the expected transitions in the modes, $|\overline{S}| = 1$ and $|\nu^2| u_0 = |u_{g0}|$, which appear in that order. The dotted curves give the imaginary components of Eqs. (13), (15), and (19). The exact positions of the theoretically predicted modes are given by open circles, labeled with the mode name. The HE_{11} mode clearly does not appear in the numerical solution. The first point is at (2.389, 0.1740), coinciding almost exactly with the theoretical prediction for the HM_{11} mode of (2.399, 0.1738). Neglecting $\overline{S}$ in Eq. (15) would give $u_\Re = 2.405$, showing that this solution is an improvement over the results of Marcatili and Schmeltzer [10] and Cros *et al.* [11], if only marginally so for this mode. The next point is at (5.155, 0.4184), corresponding to the HE_{12} mode (5.208, 0.3906), the approximation is not as good this time, the main error being the underestimate of $u_\Im$, which is the case for all of the electric modes. The adjacent point (5.403, 0.3766) is clearly the HM_{12} mode (5.441, 0.3895), again the theoretical model gives good agreement. Marcatili and Schmeltzer and Cros *et al.* give just one point in this region at (5.520, 0.3895). For the subsequent modes these models breakdown completely. For $u_0 > 6.089$ we have $|\overline{S}| > 1$, and we can clearly see the separation of the modes into transverse electric and transverse magnetic, though we only switch models for the magnetic modes. The theoretical prediction for the HE_{13} mode is (8.536, 0.3953), close to that for the TE_{13} mode (8.536, 0.3616), and closer to the numerical result of (8.522, 0.4012). We still label the mode as transverse electric because the transverse magnetic component of the fields is small. For the subsequent transverse electric modes, TE_{14}, TE_{15}, and TE_{16}, both equations give essentially the same results: (11.71, 0.4802), (14.86, 0.5627), and (18.02, 0.6333), close to the numerical points at (11.69, 0.5120), (14.84, 0.6277), and (17.99, 0.7391). The main error is the underestimate of $u_\Im$, which increases with u_0. This is to be expected, as the theory assumes $u_0 \ll |u_{g0}|$ and $u_0/|u_{g0}|$ increases with u_0. However, for the last, propagating, transverse electric mode TE_{16}, $u_0/u_{g0} = 0.6274$ and the result for $u_\Im$ is still within 15% of the numerical value. The first transverse mode is at (8.290, 0.9664), corresponding to the predicted TM'_{13} mode (8.536, 0.8136), the HM_{13} mode would be at (8.538, 0.7802). The theoretical model is

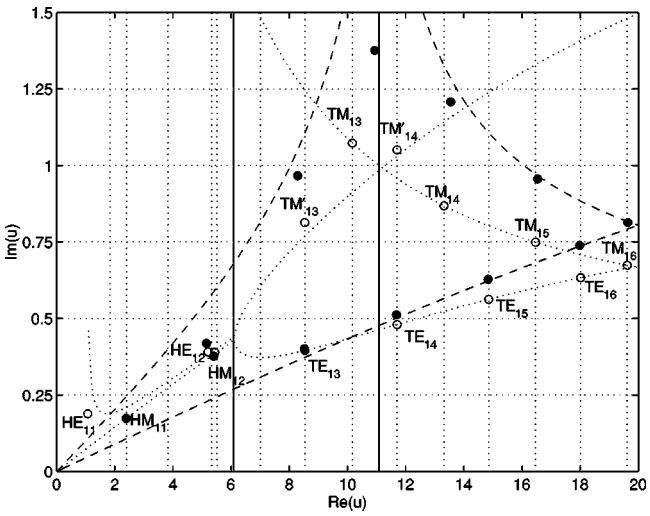

FIG. 1. Mode structure for the $n = 1$ modes in a cylindrical waveguide with $\nu = 1.5$ and $ka = 20$.

not accurate here as it assumes $|\nu^2|u_0 \ll |u_{g0}|$ and we have $\nu^2 u_0/u_{g0}=0.8025$, but it is more accurate than might be expected. For larger values of ka the theoretical model did give accurate predictions for the first few TM'_{nm} modes. In this case there are no further TM'_{1m} modes. The value of $u_{\Re}$ of the TM'_{nm} modes and the TE_{nm} modes is slightly overestimated. There is a negative, second order, contribution to $\Delta u_{\Re}$, the leading term of which is $\Delta u_{\Im}^2/u_0$ [8]. The difference is thus greater for the TM'_{nm} modes and they have lower values of $u_{\Re}$ than the TE_{nm} modes. The extension of the theory to second order, though possible, is beyond the scope of this paper. For $u_0>11.09$ we have $|\nu^2|u_0>|u_{g0}|$, so we expect the next transverse magnetic mode to be the TM_{14} mode. As expected, the TM_{13} and TM'_{14} modes do not appear, but there is a point at (10.94, 1.376), almost exactly on the transition line, which is not predicted by the theory. It is clearly a magnetic mode, but it does not fit into the predicted series of hybrid and transverse modes, so we christen it the M mode. To find an approximate solution for this M mode we use the large argument approximation for $J'_n(u)/J_n(u)$ in Eq. (6) as well as for $H'_n(u_g)/H_n(u_g)$. Assuming $|u_{\Im}| \gg 1$ we have $J'_n(u)/J_n(u) \approx -i$ giving $\nu^2 u \approx u_g$. This correctly predicts the value of $u_{\Re}$, but does not give the value of $u_{\Im}$. It only correctly determines the value of $u_{\Im}$ for large, complex refractive indices. We were unable to obtain a simple, analytic result for the M mode with a wider regime of validity. The points at (13.55, 1.208), (16.54, 0.9564), and (19.64, 0.8140) are clearly the TM_{14}, TM_{15}, and TM_{16} modes, which, according to Eq. (13), have u equal to (13.32, 0.8683), (16.47, 0.7494), and (19.62, 0.6740). This time the values of $u_{\Re}$ are slightly underestimated, the second order contribution to $\Delta u_{\Re}$ is positive for the TM_{nm} modes, and the values of $u_{\Im}$ are significantly underestimated. The approximation improves with increasing u_0 as it assumes $|\nu^2|u_0 \gg |u_{g0}|$, which is never satisfied: the last, propagating, transverse magnetic mode TM_{16} has $\nu^2 u_0/u_{g0}=1.484$. Clearly the values of $u_{\Im}$ for the magnetic modes in the vicinity of $|\nu^2|u_0=|u_{g0}|$ cannot be obtained from a theory that assumes $|\Delta u| \ll 1$. Despite this, the theory correctly predicts the rise and fall in $u_{\Im}$ and the position of the peak value, and is at least within a factor of 1.4 of the numerical values. The value of $u_{\Re}$ is accurately predicted for all of the modes.

It is interesting to see how small ka has to be in order to have a TE_{11} mode. The condition $|\overline{S}|>1$ requires $ka<0.94$, and in this case we do not expect to have any propagating modes. Requiring the HM_{11} mode to be cutoff gives $ka<2.4$. Numerical solutions showed obviously TE_{11} modes up to $ka=2.5$, where we obtained (1.841, 0.8110) compared to the theoretical prediction [Eq. (11)] of (1.841, 0.7803). For this case the hybrid electric result [Eq. (19)] is clearly not a better approximation. For the HM_{11} mode to exist we require $|\nu^2|u_0<|u_{g0}|$, giving $ka>4.34$. Numerical solutions only clearly corresponded to the HM_{11} mode at $ka=11$, where we obtained (2.351, 0.3120) compared to the theoretical prediction of (2.387, 0.3118). For intermediate values of ka there still existed a solution: as ka increased $u_{\Re}$ and $u_{g0}u_{\Im}$ increased steadily, moving between the predicted TE_{11} and HM_{11} results. This is the M mode, but the large argument approximation is not valid in this case. This is suggestive as to what might occur to the TE_{11} mode when it ceases to exist. Consider a waveguide with a slowly increasing radius that only allows the TE_{11} mode to enter. After a relatively small increase in the radius this mode ceases to exist. A mode being cutoff or reflected by a slowly increasing radius is counter intuitive, it seems likely that it is distorted as it propagates, eventually coupling to the HM_{11} mode. More generally speaking, it appears likely that the $m=1$ transverse electric components and the lower-order transverse magnetic components of an arbitrary electromagnetic wave, propagating in a waveguide that does not support these modes, will be distorted by the losses, eventually coupling to the hybrid modes.

Our previous model [8] gives $u_{\Im}$ in terms of a reflectivity R that is a specified function of angle of incidence and polarization. Ignoring the complications of obtaining an averaged angle of incidence and polarization, it gives $u_{\Im}=-\ln(R)/4$, the angle of incidence ϕ is given by $\sin\phi=u_{\Re}/ka$, the transverse electric modes are s polarized and the transverse magnetic modes are p polarized. The values of $u_{\Im}$ given by this expression, using the full Fresnel equations [8], are shown as dashed lines in Fig. 1, the p-polarized reflectivity giving the higher value. The values of $u_{\Im}$ for the transverse modes are accurately reproduced. The values for the hybrid modes lie between the s- and p-polarized results. Only the values of $u_{\Im}$ for the TM'_{13} and TM_{14} modes are slightly overestimated at 1.051 and 1.284, respectively, compared to the actual values of 0.9664 and 1.208. However, the value of $u_{\Im}$ for the M mode, which coincides almost exactly with the peak in $u_{\Im}$, is considerably overestimated at 2.590, compared to the actual value of 1.376. This model, though more accurate than that described here for the transverse modes, still breaks down for the magnetic modes in the vicinity of $\nu^2 u=u_g$, or in terms of the reflectivity near the minimum in the p-polarized reflectivity. Including the f_ψ term [8], which takes account of the varying angle of incidence and polarization, gave even better agreement with the transverse electric results and made no significant difference to the transverse magnetic results.

Finally, we briefly consider a complex refractive index $\nu=3.53-4.1i$, again for $ka=20$ and $n=1$. The results are given in Fig. 2, in exactly the same format as the previous results. This refractive index is the upper limit for aluminum at a wavelength of 1 μm that we considered in our previous paper [8]. We have not extensively investigated complex refractive indices, so we do not know if these results are typical. In this case the refractive index is almost sufficient to obtain the loss-less mode structure. There are no TM'_{1m} modes and only one hybrid mode, the HM_{11} mode. This mode occurs near $|\nu^2|u_0=|u_{g0}|$, and we see the breakdown of the hybrid magnetic solution. The theoretical prediction for the HM_{11} mode is (2.676, 0.3381), and the numerical result is (2.687, 0.4371). The value of $u_{\Re}$ is accurately predicted, but $u_{\Im}$ is significantly underestimated. The next point (indicated by an arrow) is off the top of the figure at (2.814, 2.048), this is the M mode. Using the large argument

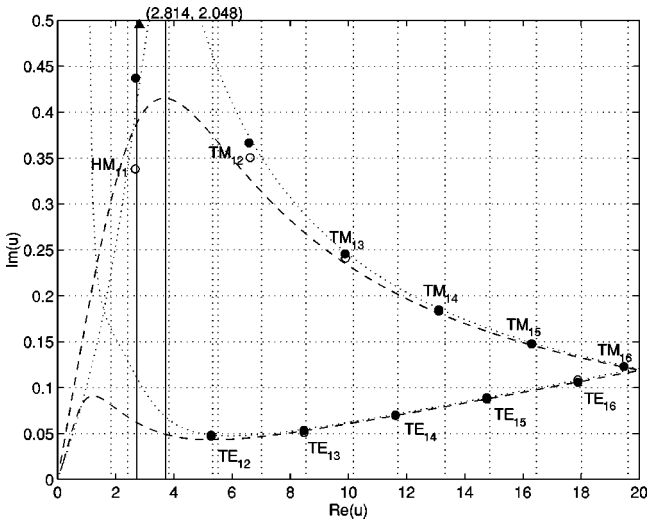

FIG. 2. Mode structure for the $n=1$ modes in a cylindrical waveguide with $\nu=3.53-4.1i$ and $ka=20$.

solution, $\nu^2 u \approx u_g$, gives (2.465, 2.786). The relatively large error is not surprising, considering that $J_n'(u)/J_n(u)$ at the numerically determined point is $-0.1202,-0.8793i$, not $-i$ as is assumed. The next point is at (5.274, 0.04720), as $|\overline{S}|>1$ we identify this as the TE_{12} mode, but we use the HE_{12} prediction [Eq. (19)] of (5.273, 0.04835), which gives much better agreement than the TE_{12} prediction [Eq. (11)] of (5.292, 0.03263). Equation (19) also gives marginally better agreement for the TE_{13} mode. For the subsequent transverse electric modes Eqs. (11) and (19) give almost identical results, but Eq. (11) did give marginally better agreement this time. For this higher-refractive index the approximations $u_0 \ll |u_{g0}|$ and $|\nu^2|u_0 \gg |u_{g0}|$ are more accurate and the theoretical results are in good agreement with almost all of the numerical results. Only the TM_{12} prediction is slightly out at (6.620, 0.3505) compared to the numerical result of (6.578, 0.3666). The value of $|\nu^2|u_0/|u_{g0}|$ for this mode is only 1.489, so the agreement is better than would be expected. It is interesting to note that the values of $u_\Im$ for this mode and for the HM_{11} mode are accurately determined by using the predicted value of $u_\Re$ in place of u_0 to calculate $u_\Im$. This clearly indicates that a second-order treatment would accurately predict the results, but it is not sufficient to indicate if substituting $u_\Re$ for u_0 would, in general, give better predictions for $u_\Im$. The values of $u_\Re$ are more accurately predicted than in dielectrics as there is now a first-order contribution to $\Delta u_\Re$.

We also examined this case using the reflectivity model. This time it was necessary to include the f_ψ term to give accurate results for the transverse electric modes. The results are very close to the numerical results for the transverse modes and very similar to those of the current model, however, in this case they are not more accurate. In the context of the reflectivity model, the fact that the hybrid solution [Eq. (19)] gives better agreement with the numerical results than the transverse solution [Eq. (11)] is due to the inherent mixed polarization of the $n>0$ transverse electric modes. The reflectivity model again fails in the vicinity of $|\nu^2|u_0=|u_{g0}|$, this time underestimating $u_\Im$. For the HM_{11} mode even the *p*-polarized reflectivity gives a value of $u_\Im$ lower than the numerical value 0.3857 compared to 0.4371, for the *M* mode it is much lower at 0.3933 compared to 2.048, and for the TM_{12} mode the result is still somewhat low at 0.3284 compared to 0.3666. This leads to an interesting conclusion: the *p*-polarized reflectivity of a curved surface is lower than that of a plane surface in metals and plasmas and higher in dielectrics.

From these examples we can conclude that the theoretical model is adequate for the vast majority of modes, and that it is more accurate for larger, complex refractive indices. The theory only proves inadequate in calculating the losses ($u_\Im$) for the magnetic modes in the vicinity of $|\nu^2|u_0=|u_{g0}|$. The examples show an additional magnetic mode, the *M* mode, in this region. Assuming that $|u_\Im| \gg 1$ we obtained $\nu^2 u \approx u_g$ for this mode, which has been seen to be of limited validity.

VI. CONCLUSIONS

We have established two parameters that determine the mode structure in cylindrical waveguides, $|\overline{S}|$ [Eq. (17)] and $|\nu^2|u_0/|u_{g0}|$. The value of these parameters increases with the refractive index and the mode order, and exceeds 1 in all waveguides, at least for the higher-order modes. For $|\overline{S}|<1$ we have hybrid electric, HE_{nm}, and hybrid magnetic modes, HM_{nm}. For $|\overline{S}|>1$ we have transverse electric, TE_{nm}, and transverse magnetic modes, TM_{nm}, as in the loss-less case. For $n=0$, $|\overline{S}|$ goes to infinity and the modes are identically transverse. For $|\nu^2|u_0/|u_{g0}|<1$ the transverse magnetic modes have significantly lower values of u_0 than in the loss-less case, equal to those of the corresponding transverse electric modes. We introduced the notation TM_{nm}' to distinguish these modes. For $|\nu^2|u_0/|u_{g0}|>1$ the mode structure is the same as in the loss-less case. The three different regimes of the magnetic modes required three different, approximate, solutions [Eqs. (12), (13), and (15)]. None of these solutions are accurate in the vicinity of $|\nu^2|u_0/|u_{g0}|=1$, where they underestimate the losses. Numerical solutions showed an additional magnetic mode near this transition, which we called the *M* mode. We obtained an approximate solution for this mode, $\nu^2 u \approx u_g$, assuming $|u_\Im| \gg 1$, which is of limited validity. We obtained approximate solutions for the transverse electric [Eq. (11)] and hybrid electric modes [Eqs. (19) and (20)], which have been found to be adequate for all cases of interest. For the $n>0$ electric modes the hybrid solution accurately describes all except the $m=1$ modes. There are no $m=1$ hybrid electric modes. The transverse solution is required to describe the $m=1$ transverse electric modes and the $n=0$ modes. The changes to the loss-less mode structure mean that we do not have a complete set of orthogonal modes, and hence that we do not have a general solution to Maxwell's equations.

This work forms a bridge between previous hybrid solutions [10,11] and loss calculations based on the loss-less modes [8,9], which are seen to be different limits of the problem.

Finally, we consider the implications for our previous model [8]. It is valid for modes with $|\nu^2|u_0>|u_{g0}|$, or in terms of the reflectivity, when the *p*-polarized reflectivity increases with increasing incidence angle. However, taking into account the change in u_0 of the transverse magnetic modes when $|\nu^2|u_0<|u_{g0}|$, it can be applied to $n=0$ modes and $n>0$ modes with $|\overline{S}|>1$, which are less restrictive conditions. However, it is not valid for transverse magnetic modes near $|\nu^2|u_0=|u_{g0}|$, that is, near the minimum in the *p*-polarized reflectivity. This can be associated to significant changes in the *p*-polarized reflectivity for curved surfaces; the model treats the guide wall, point by point, as a plane surface. The validity of the model for $n=0$ and $|u|\gg n$ can be explained by the fact that in these cases the guide wall can be treated as a plane surface. For $n=0$ this is because the fields are identical at every point around the wall. For $|u|\gg n$ the large argument approximation for the Bessel functions is valid and in this limit the fields at the wall have the same form as a plane wave. The validity of the model for high-refractive indices can be explained by the negligible penetration of the fields in the guide wall [9]. We have seen that it is more accurate for the transverse modes in dielectrics than the model given here and that it gives similar results for metals and plasmas. This indicates that it could be applied to plasma waveguides where the assumptions used here do not apply, but the reflectivity is known from other theoretical or experimental results.

ACKNOWLEDGMENT

J.R.D. was supported by a grant from the Fundação para a Ciência e a Tecnologia.

[1] M. Borghesi, A.J. Mackinnon, R. Gaillard, O. Willi, and A.A. Offenberger, Phys. Rev. E **57**, R4899 (1998).
[2] M. Nisoli, S. De Silvestri, and O. Svelto, Appl. Phys. Lett. **68**, 2793 (1996).
[3] C.G. Durfee III, A.R. Rundquist, S. Backus, C. Herne, M.M. Murnane, and H.C. Kapteyn, Phys. Rev. Lett. **83**, 2187 (1999).
[4] F. Dorchies, J.R. Marquès, B. Cros, G. Matthieussent, C. Courtois, T. Vélikoroussov, P. Audebert, J.P. Geindre, S. Rebibo, G. Hamoniaux, and F. Amiranoff, Phys. Rev. Lett. **82**, 4655 (1999).
[5] C. Stöckl and G.D. Tsakiris, Laser Part. Beams **9**, 725 (1991).
[6] B. Rau and R.A. Cairns, Phys. Plasmas **7**, 3031 (2000).
[7] S. Jackel, R. Burris, J. Grun, A. Ting, C. Manka, K. Evans, and J. Kosakowskii, Opt. Lett. **20**, 1086 (1995).
[8] J.R. Davies and J.T. Mendonça, Phys. Rev. E **62**, 7168 (2000).
[9] R. S. Elliot, *An Introduction to Guided Waves and Microwave Circuits* (Prentice-Hall International, Englewood Cliffs, 1993).
[10] E.A.J. Marcatili and R.A. Schmeltzer, Bell Syst. Tech. J. **43**, 1783 (1964).
[11] B. Cros, C. Courtois, G. Matthieussent, A. Di Bernardo, D. Batani, N. Andreev, and S. Kuznetsov, Phys. Rev. E **65**, 026405 (2002).
[12] MATLAB Version 6.0.0.88, Release 12, The MathWorks Inc., 2000.